THE UNIVERSITY of EDINBURGH

Edinburgh Research Explorer

The importance of laboratory water quality for studying initial bacterial adhesion during NF filtration processes

Citation for published version:
Semiao, AJC, Habimana, O, Cao, H, Heffernan, R, Safari, A & Casey, E 2013, 'The importance of laboratory water quality for studying initial bacterial adhesion during NF filtration processes', *Water Research*, vol. 47, no. 8, pp. 2909-2920. https://doi.org/10.1016/j.watres.2013.03.020

Digital Object Identifier (DOI):
10.1016/j.watres.2013.03.020

Link:
Link to publication record in Edinburgh Research Explorer

Document Version:
Early version, also known as pre-print

Published In:
Water Research

General rights
Copyright for the publications made accessible via the Edinburgh Research Explorer is retained by the author(s) and / or other copyright owners and it is a condition of accessing these publications that users recognise and abide by the legal requirements associated with these rights.

Take down policy
The University of Edinburgh has made every reasonable effort to ensure that Edinburgh Research Explorer content complies with UK legislation. If you believe that the public display of this file breaches copyright please contact openaccess@ed.ac.uk providing details, and we will remove access to the work immediately and investigate your claim.

OPEN ACCESS

Download date: 26. Apr. 2024

The importance of laboratory water quality for studying initial bacterial adhesion during NF/RO filtration processes

A.J.C. Semião [§], O. Habimana [§], H. Cao, R. Heffernan, A. Safari, E. Casey [*]

School of Chemical and Bioprocess Engineering, University College Dublin (UCD), Belfield, Dublin 4, IRELAND

[§]Both authors contributed equally to this work

*Corresponding author. Mailing address: University College Dublin, School of Chemical and Bioprocess Engineering, Belfield, Dublin 4, IRELAND. Phone: +353 1 716 1974. Email: eoin.casey@ucd.ie

Keywords: Compaction, water quality, cell adhesion, nanofiltration

Abstract

Biofouling of nanofiltration (NF) and reverse osmosis (RO) membranes for water treatment has been the subject of increased research effort in recent years. A prerequisite for undertaking fundamental experimental investigation on NF and RO processes is a procedure called compaction. This involves an initial phase of clean water permeation at high pressures until a stable permeate flux is reached. However water quality used during the compaction process may vary from one laboratory to another. The aim of this study was to investigate the impact of laboratory water quality during compaction of NF membranes. A second objective was to investigate if the water quality used during compaction influences initial bacterial adhesion.

Experiments were undertaken with NF270 membranes at 15 bar for permeate volumes of 0.5L, 2L, and 5L using MilliQ, deionized or tap water. Membrane autopsies were performed at each permeation point for membrane surface characterisation by contact angle measurements, profilometry, and scanning electron microscopy. The biological content of compacted membranes was assessed by direct epi-fluorescence observation following nucleic acid staining. The compacted membranes were also employed as substrata for monitoring the initial adhesion of *Ps. fluorescens* under dynamic flow conditions for 30 minutes at 5 minutes intervals.

Compared to MilliQ water, membrane compaction using deionized and tap water led to decreases in permeate flux, increases in surface hydrophobicity and led to significant build-up of a homogenous fouling layer composed of a both living and dead organisms ($>10^6$ cells.cm^{-2}). Subsequent measurements of bacterial adhesion resulted in cell loadings of 0.2×10^5, 1.0×10^5 cells×cm^{-2} and 2.6×10^5 cells.cm^{-2} for deionized, tap water and MilliQ water

43 respectively. These differences in initial cell adhesion rates demonstrate that choice of
44 laboratory water can significantly impact the results of bacterial adhesion on NF
45 membranes. Standardized protocols are therefore needed for the fundamental studies of
46 bacterial adhesion and biofouling formation on NF and RO membrane. This can be
47 implemented by first employing pure water during all membrane compaction
48 proceduresand for the modelled feed solutions used in the experiment
49

50 **1 Introduction**

51 Nanofiltration (NF) and reverse osmosis (RO) membranes are commonly used for the
52 removal of organic matter and trace contaminants, such as pesticides, during water
53 treatment processes (Cyna et al. 2002). The efficiency of NF and RO processes is however
54 adversely affected by membrane biofouling (Flemming 1997, Ivnitsky et al. 2007), principally
55 due to the formation of biofilms (Flemming 2002). These ecosystems are usually made up of
56 a community of dead and living microorganisms held together by a matrix of
57 polysaccharides, lipids, proteins, organic matter, amongst other components (Flemming
58 2002). Biofilms are ubiquitous in NF and RO membrane plants (Houari et al. 2009,
59 Vrouwenvelder et al. 1998, Vrouwenvelder et al. 2008, Khan et al. 2013) and are the Achilles
60 heel of NF and RO processes (Flemming et al. 1997) as they are difficult to remove (Hijnen et
61 al. 2012). Biofouling increases pressure drop along the membrane module (Vrouwenvelder
62 et al. 2009a, Hijnen et al. 2009), leading to increased costs associated with energy
63 consumption. The presence of biofilms on the membrane surface has also been shown to
64 significantly affect permeate flux, and solute retention (Ivnitsky et al. 2005, Huertas et al.

2008). The decrease in solute retention and permeate flux has been attributed to enhanced concentration polarisation caused by the biofilms (Herzberg and Elimelech 2007). It has been shown that the concentration polarization also maintains the presence of biofilms by concentrating nutrients from the bulk environment (Chong et al. 2008, Vrouwenvelder et al. 2009b).

Biofilm formation is initiated by the irreversible adhesion of bacterial cells onto the membrane's surface, which is influenced by a number of factors. Firstly, the cell properties such as hydrophobicity (Ridgway et al. 1985) and cell surface 76 charge (Subramani and Hoek 2008) have been found to affect adhesion. Secondly, the membrane physicochemical properties (roughness, charge and hydrophobicity) have been shown to impact the degree of adhesion. In general, the rougher and the more hydrophobic the membrane is, the more cells will adhere to the surface (Subramani and Hoek 2008, Myint et al. 2010, Khan et al. 2011)**.** Finally, the presence of a conditioning layer on the membrane also affects bacterial adhesion (Subramani et al. 2009). A recent study has shown that a conditioning layer of salts and organic carbon promoted a homogeneous biofilm, whilst the absence of a conditioning layer resulted in a scattered and thin biofilm (Baek et al. 2011).

The intractable nature of the biofouling problem has led to a significant increase in research in this area in recent years (Herzberg and Elimelech 2007, Chong et al. 2008, Subramani and Hoek 2008, Baek et al. 2011, Fonseca et al. 2007). These studies range from the effects of biofilms on process performance (Ivnitsky et al. 2005, Huertas et al. 2008) to biofouling control through the design of antifouling membranes (Miller et al. 2012, Bernstein et al. 2011).

Although membrane biofouling research methodologies differ from one research laboratory to another, they generally share a common pre-treatment procedure involving the

compaction of the studied membrane prior to biofouling experiments. To accurately monitor flux changes and solute retention during NF and RO experiments caused by osmotic pressure or membrane fouling, membranes are purposely compacted to prevent changes due to the effect of pressure during the experiment. The compaction of NF and RO membranes is carried out under different filtration conditions depending on the laboratory they are carried out. The compaction is typically undertaken at a pressure between 6 and 25 bar and up to 18 hours in duration (Herzberg and Elimelech 2007, Baek et al. 2011, Fonseca et al. 2007, Suwarno et al. 2012). This translates into a 99 typical water permeation volume between 2 L (membrane flux=50 $L.h^{-1}.m^{-2}$, time=18 hours and 22.44 cm^2 100 membrane area) and 15 L (membrane flux=65 $L.h^{-1}.m^{-2}$, time=12 hours and 186 cm^2 101 of membrane area) (Baek et al. 2011, Suwarno et al. 2012) calculated as: $V(L)=Flux(L/h.m^2)\times time(h)\times Membrane\ Area(m^2)$.

Although membrane compaction is a prerequisite to most NF and RO experimental studies, including bioadhesion/biofouling, the type of water used to compact the membrane may vary considerably from one laboratory to another. The water used in recent published studies on initial adhesion and biofouling experiments spans from non-sterilised tap water (Hijnen et al. 2009, Khan et al. 2011, Vrouwenvelder et al. 2009c, Vrouwenvelder et al. 2007,Botton et al. 2012, Khan et al. 2010), DI water (Huertas et al. 2008, Herzberg and Elimelech 2007, Myint et al. 2010, Baek et al. 2011, Lee et al. 2010) and MilliQ water (Chong et al. 2008, 2007, Pang et al. 2005). Tap water and DI water will vary in quality depending on the water source and the yearly season (Gibbs et al. 1993). In essence, the total carbon, biological and endotoxin contents will differ from one water type to another, whether the water is sterilized or not. Moreover, when considering filtration aspects, all insoluble water constituents will most certainly be deposited on the membrane surface during the

compaction, thus altering the membrane surface from its original state. The conditioning layer formed during the compaction pre-treatment of NF/RO is likely to result in altered surface characteristics thereby affecting subsequent biofouling experiments.

The objective of this study was to first demonstrate the impact of the choice of water used during compaction of NF membranes in terms of membrane performance, surface characterisation and secondly, to investigate whether the 121 water used during membrane compaction also affects bioadhesion outcomes.

2 Materials and Method

2.1 Water source and characterisation

Three different water grades were used in our study: tap water provided by south Dublin water municipality, deionized water obtained by a purifying water system (Elgastat B124, Veolia, Ireland) and Grade 1 pure water (18.2 $M\Omega.cm^{-1}$) obtained by an Elga Process Water System (Biopure 15 and Purelab flex 2, Veolia, Ireland), hereafter referred to as MilliQ water. Conductivity and pH measurements were performed on all water samples at room temperature (20° C) and total organic carbon of all water samples was determined using a total organic carbon analyser (TOC-VCSH, Shimadzu, Ireland) in the NPOC mode, equipped with an automatic sample injector and an NDIR detector. Calibration standards were made using potassium hydrogen phthalate at different concentrations between 0 and 10 mgC/L.

The water samples were collected in new 50 mL sterile Eppendorf tubes, filtered twice with

133 polyethersulphone 0.2 µm filters (Corning Incorporated, VWR Ireland), put in TOC vials that
134 had been soaked overnight in 0.5 M NaOH in MilliQ water and left to dry at 30°C upside
135 down to avoid any contamination from the air followed by a thorough rinsing with MilliQ
136 water and analysed straight away. Measurement results are presented in Table 1. The
137 measurements were carried out from samples taken between October and November 2012.
138 In the particular case of MilliQ water, the samples have a measured TOC concentration that
139 varied from 0.00 to 0.24 $mgC.L^{-1}$. The average value measured for 10 samples were
140 0.13±0.06 $mgC.L^{-1}$ (Table 1).
141 The total solids were measured by filling a glass vial with 40 mL of each water source and
142 allowing it to evaporate in an oven at 100°C. The vial weight was measured before and after
143 evaporation and the difference obtained in weight corresponded to the total solids weight.
144 A control sample was used, where an empty vial was placed in the oven to ensure no
145 floating particles present could affect the results.

146 The pH was measured with a HI1332 pH probe (Hannah, VWR, Ireland) and the conductivity
147 was measured with a TetraCon 325 conductivity probe (WTW, VWR, Ireland).

148 The total amount of cells in each water source was determined as follows: a volume of 100
149 mL of MilliQ and tap water and 80 ml of DI water were filtered with a 0.2 µm filter (GTBP-
150 25mm, Millipore, Ireland). The filter was then removed, placed in 3 mL of raw water without
151 carbon (as explained in section 2.3.1) and stained with SYTO® 9 and PI dyes. The filter was
152 then observed under an Epi-fluorescence microscope (Olympus BX 51) using a 40x objective.
153 Fluorescent organisms were observed using two filter cubes each exciting SYTO® 9 and PI
154 dyes at 450 nm and 550 nm respectively. At least ten micrographs were obtained at 5

155 random points on each compacted stained membrane sample. The number of fluorescent
156 organism were then counted using Image J® (NIH, Bethesda, MD, USA).

157

158

159 2.2 Compaction experiment

160 NF 270 membranes (Filmtec Corp. USA) were used as the reference nanofiltration
161 membrane in this study. The membranes were gently washed and left soaking overnight in
162 the fridge in the water source they were going to be exposed to during the experiment in
163 order to remove all the preservatives. The membrane compaction experiments were
164 performed in Membrane Fouling Simulators (Vrouwenvelder et al. (2006)) at 15 bar
165 pressure and a feed flow rate of 0.66L/min in each cell using one type of water grade for
166 each experimental run. This flow rate corresponds to a velocity of 0.35 m/s, a Re_{dh} of 579
167 and a shear rate of 2588 s^{-1} in each cell.
168 The cross-flow system was equipped with a 10 L autoclavable feed tank (Nalgene, VWR
169 Ireland) and a high pressure pump (P200 from Hydra-Cell, UK). The system was connected to
170 three MFS devices placed in parallel holding each NF 270 membranes on the experimental
171 rig at the start of compaction. The MFS cells are of the slit type channel height of 0.8 mm,
172 width of 40 mm and length of 255 mm. Each membrane cell holds a membrane of 102 cm^2.
173 Separate experiments were carried out in the cross-flow system in order to confirm that the
174 feed flow rate was distributed evenly by the three cells. The pressure on the outlet side of
175 the slit feed channel of each of the 3 membrane cells was measured during operation at
176 different flow rates and pressures. The pressure between the different MFS cells did not
177 vary by more than 2% for the conditions tested, showing that the flow rate distributes

evenly in the system. Temperature was monitored in the feed tank with a temperature indicator (Pt 100, Radionics, Ireland) and maintained at 20ºC ± 1ºC with a coil inside the tank connected to a temperature controlled MultiTemp III water bath (Pharmacia Biotech, Ireland). A back pressure regulator (KPB1L0A415P20000, Swagelok, UK) allows the pressurization of the system. The pressure was monitored in both feed and retentate side of the membrane cells with two pressure transducers (PTX 7500, Druck, Radionics, Ireland). The feed flow was measured using a flow meter (OG2, Nixon Flowmeters, UK). Datalogging was set-up for monitoring inlet and outlet pressure, feed flow rate and temperature (PicoLog 1000, PicoTechnology, Radionics, Ireland). The permeate volume collected was measured using 1000 mL graduated bottle, where the permeate volume was not returned to the feed tank. The permeate flux was determined by measuring a volume of permeate with a balance HCB123 balance (Adams, Astech Ireland) with a stopper. The P&ID of the crossflow filtration system is depicted in Figure 1.

Permeate flux and permeate conductivity measurements were performed throughout the compaction experiment. Once permeate levels reached 0.5L for each MFS device, the compaction was temporarily stopped to allow removal of one MFS device from the rig. Compaction was thereafter continued for the two remaining MFS devices until permeate levels reached 2L levels each, at which point the second MFS was removed from the system. The last MFS was left compacting until 5L permeate was collected.

Once removed from the rig system, the MFS device containing a compacted NF270 membrane was opened while submerged under the corresponding water type. Membrane

samples were immediately cut to size for autopsy and dynamic adhesion experiments as described in sections 2.2.1.4 and 2.3.2. The remainder of the membrane was left to dry in a closed box at room temperature for at least 48 hours to ensure the membrane was dry.

2.2.1 Surface characterisation assays of compacted NF270 membranes.

2.2.1.1 Profilometry

Optical profilometery analysis was carried out to examine the morphology and to quantify surface roughness. These measurements were carried out using a Wyko NT1100 optical profilometer operating in vertical scanning interferometry (VSI) mode. The R_q (root mean square roughness) was obtained on three different locations on each sample surface and an average value obtained.

2.2.1.2 Contact angle measurements

The Lifshitz-van der Waals (γ^{LW}), electron-donor (γ^-) and electron-acceptor (γ^+) surface tension components of dehydrated compacted NF 270 membrane samples (S) were determined by measuring contact angles using the following expression:

$$cos\theta = -1 + 2\,(\gamma_S^{LW}\gamma_L^{LW})^{\frac{1}{2}}/\,\gamma_L + 2\,(\gamma_S^{+}\gamma_L^{-})^{\frac{1}{2}}\,/\gamma_L + 2\,(\gamma_S^{-}\gamma_L^{+})^{\frac{1}{2}}/\gamma_L \quad (1)$$

Contact angles (ϑ) and surface energy measurements (γ^S) of dehydrated compacted NF 270 membrane were measured at room temperature using a goniometer (OCA 20 from Dataphysics Instruments) with three static pure liquids (L): deionised water, diiodomethane and ethylene glycol.

The Lewis acid-base component was deduced from:

$$\gamma_S^{AB} = 2\sqrt{(\gamma_S^+ \gamma_S^-)} \quad (2)$$

And the total surface energy was defined by:

$$\gamma_{S = \gamma^{AB} + \gamma^{LW}} \quad (3)$$

Contact angle values and determined surface energies values presented in table 2 represent the mean of at least 10 measurements per compacted sample membrane. Contact angle measurements were repeated in two independent replicates.

2.2.1.3 Scanning electron microscopy

For high resolution *ex-situ* observations of the membrane surface, the compacted NF 270 membranes were dehydrated by drying in air and then gold coated for 30 sec at x V 30 mA. High magnification imaging of the membrane surfaces was performed under a Hitachi SEM at the UCD Nano-imaging and Materials Analysis Centre.

2.2.1.4 Biological assessment of NF 270 compacted membranes

For assessing the biological presence on membranes samples, three regions of the compacted NF 270 membranes were cut and placed in small petri dishes containing 3mL of the water grade used during compaction. Membrane samples were then stained by adding 0.5 µL of 3.34mM SYTO® 9 green-fluorescent nucleic acid staining solution and 0.5 µL of 20 mM propidium iodide red-fluorescent nucleic stain. Stained membrane samples were

subsequently incubated in the dark for at least 15 minutes, after which the staining mix was discarded from the petri dish and a cover slip placed on membrane surfaces. The stained sample was then observed under an Epi-fluorescence microscope (Olympus Bx 51) using a 20x objective. Fluorescent organisms were observed using two filter cubes each exciting SYTO® 9 and PI dyes at 450nm and 550nm respectively. Ten micrographs were obtained at 5 random points on each compacted stained membrane sample. The number of fluorescent organism was then counted using Image J®, an image quantification software.

2.3 Initial adhesion assay on NF270 compacted membranes

2.3.1 Microbial strain and culture conditions

The *Pseudomonas fluorescens* NCTC 10038 was selected for dynamic adhesion assays on compacted NF 270 membrane. The cells were stored at -20°C with 20% volume glycerine as a cryoprotectant. Prior to experiments, cells were spread on King B agar (Oxoid) and incubated at 30°C overnight. Single colonies were then inoculated in were then cultured at 30°C and 150 rpm in Raw Water (RW) medium (tryptic soy broth 0.3 $g.L^{-1}$, sodium citrate $Na_3C_6H_5O_7$ 0.26 $g.L^{-1}$, $NaHCO_3$ 0.042 $g.L^{-1}$, NaCl 0.12 $g.L^{-1}$, KH_2PO_4 0.063 $g.L^{-1}$, $MgSO_4$ 0.15 $g.L^{-1}$, NH_4Cl 0.005 $g.L^{-1}$, $CaCl_2$ 0.076 $g.L^{-1}$). When cell density reached 0.270 at OD_{600}, 12mL of the overnight culture were centrifuged at 7000 rpm for 10 minutes, before discarding supernatant. The remaining pellet was suspended with Raw Water medium containing no C-source (RW^{-C}) to a final volume of 1 mL. The cells were then stained by adding 0.5 µL of 3.34mM SYTO® 9 and 0.5 µL of 20 mM propidium iodide, followed by a 15 minutes incubation period at room temperature in the dark. The stained *Ps. fluorescens* cells were then centrifuged at 7000 rpm for 10 min before discarding the supernatant. The remaining

pellet was then re-suspended in 24 mL RW^{-C} medium prior to adhesion experiments order to attain a final cell concentration of 10^7 cells.mL^{-1}.

2.3.2 Initial adhesion assay

Initial adhesion assays were performed on freshly cut compacted membranes that were placed on a support inserted in a flow cell (Model BST FC 81, Biosurface Technologies Corporation, Bozeman, MT) with modified channel dimensions of 0.8 by 12.7 by 47.5 mm. Compacted membranes were immobilized on the support using double sided tape, and hydration was ensured by filling the flow cell chamber with RW^{-c} prior to adhesion experiments. The flow cells are small continuous-flow systems with a glass viewing port that allowed *in situ* observation using an Epi-fluorescence microscope (Olympus BX 51) and a 20x objective. After removing bubbles from the system, "zero point" images of the NF270 compacted surface were recorded using two filters with excitation wavelengths set at λ_{ex}450nm and λ_{ex} 550nm respectively. The freshly stained 24 mL *Ps. fluorescens* cells suspension was then circulated in the system at a volumetric flow rate of 1.5 ml min^{-1}. Adhesion time was recorded after 1, 5, 10, 15, 20, 25 and 30 minutes after the first observed cell adhered on the surface. Two images were recorded at λ_{ex} 450 nm and λ_{ex} 550 nm for each time point. Images of a size of 223 µm x 1627 µm were taken and analysed by counting adhered stained *Ps. fluorescens* cells using Image J®.

The initial adhesion kinetics of *Ps. fluorescens* on compacted membranes was established for all water sources using the following equation:

$$q(t) = q_{max} \cdot (1 - e^{-\beta t}) \quad (4)$$

where *q(t)* is the bacterial loading as a function of time (*t*), the maximum cell loading q_{max}, and the accumulation factor *β* obtained by the exponential fit of the adhesion experimental data. The linear region of the obtained curve was used to calculate the rate of adhesion by using the following expression:

$$k_d = \frac{\theta(t)}{\Delta t} \cdot \frac{1}{C_0} \quad (5)$$

where, k_d is the deposition rate of *Ps. fluorescens* on NF 270 membranes, *ϑ (t)* the number of adhered cells over a time period (*Δt*) between two time points and C_0 the initial bacterial suspension feed concentration.

3 Results

3.1 Water quality assessment

The different water qualities used for compacting NF 270 membranes used in this study were characterized prior to pre-compaction experiments and are presented in Table 1.

No detectable solids were measured in MilliQ and deionized water samples used in this study. MilliQ water had the lowest pH, total organic carbon, and conductivity values compared to deionized and tap water, respectively. MilliQ water has a very low conductivity

of 0.4 µS.cm^{-1} followed by DI water with a conductivity of 4 µS.cm^{-1}. The highest conductivity obtained was for tap water with 168 µS.cm^{-1}.

No cultivable cells (determined by CFU) were found in MilliQ. However deionized water was found to contain 170 times the number of cultivable organisms found in tap water. Direct count analysis (counting both culturable and non-culturable cells) revealed the presence of significant higher amounts of microorganisms in all tested water samples. Deionized water was found to contain 1800 and 15 times more microorganisms than in MilliQ and tap water, respectively. Moreover, deionized water also contained 850 and 30 times the amounts of dead/injured microorganisms found in MilliQ and tap water, respectively.

3.2 Effects of different water grades on NF 270 membrane performance during compaction.

In order to determine how each water source impacted the permeate flux during compaction, the permeate flux was measured for 0.5, 2 and 5 L of permeated water in the MFS cells. The results are presented in Figure 2. After a volume of 0.5 L of water permeated through the membrane, membranes compacted with tap water showed the lowest permeate flux of 195 L.h^{-1}.m^{-2}.bar^{-1} compared to membranes compacted with deionized and MilliQ water, which had permeate fluxes of 283 and 339 L.h^{-1}.m^{-2}.bar^{-1} respectively. Additionally, the use of tap water during compaction led to a constant decrease in permeate flux from 195 L.h^{-1}.m^{-2}.bar^{-1} to 96 L.h^{-1}.m^{-2}.bar^{-1} with the NF 270 membrane, as permeate volume increased from 0.5 L to 5 L. Visual inspection showed that the membrane surface was light coloured at 0.5 L and gradually increased to a dark yellow colour at 5 L (not shown) for tap water. In contrast, permeate flux stabilized after 0.5 L of water permeated through

the membrane for membranes compacted with deionized and MilliQ: from 2 L to 5 L the permeate flux stabilised at 251 and 301 $L.h^{-1}.m^{-2}.bar^{-1}$, respectively.

3.3. Effect of different water grades on NF 270 membrane surface properties.

The physico-chemical properties of NF 270 compacted membranes were evaluated by contact angle measurements and the associated van der Waals (γ^{LW}), Lewis Base (γ^{-}) and Lewis Acid (γ^{+}) components are presented in Table 2. Membranes exhibited increased hydrophobic character with increased permeate volumes. Membranes compacted with 5 L of MilliQ water showed the lowest hydrophobic properties (ϑ_{water} =49.7), followed by membranes compacted with tap water (ϑ_{water} =56), and deionized water (ϑ_{water} =68.9) respectively, with the surface hydrophobicity varying in the following order: MilliQ<tap<DI water. Increasing permeate volumes can be seen to have not affected the van der Waals (γ^{LW}) character of the compacted membranes. However, membranes compacted with deionized water showed lowest van der Waal surface properties with 37 $mJ{\bullet}m^{-2}$ compared to membranes compacted with MilliQ (42.3 $mJ{\bullet}m^{-2}$) and tap (45.5 $mJ{\bullet}m^{-2}$) water respectively. A significant decrease in Lewis Base (γ^{-}) membrane character was noticeable from 2L to 5L permeation using MilliQ water, whereas the same drop in Lewis base properties occurred earlier from 0.5L to 2L in membranes compacted with deionized and tap water. Membrane Lewis Acid (γ+) character decreased by 2.5 fold from 0.5L and 2L permeated volumes of MilliQ, and during 2L to 5 L permeated volumes of deionized water. A 13.7 fold increase of Lewis Acid (γ^{+}) character was observed in compacted membrane after permeation of 2L to 5L tap water.

Roughness measurements of the different compacted membranes measured by optical profilometry are also presented in Table 2. No significant differences in surface roughness were observed for compacted membranes after permeation of 0.5L and 2L MilliQ, deionized water, and tap water. Although no differences in surface roughness were observed for membranes compacted with MilliQ (511 ± 143 nm) and deionized water (562 ± 123 nm) after 5 L permeation, membranes compacted with tap water showed highest roughness with 1166 ± 147 nm. Height topography results presented in Figure 3 showed that the surface of compacted membranes using MilliQ water (Figure 3 A) showed areas of very smooth surface topology profiles and areas with irregular and heterogeneous surface topology profiles, due to what looked like surface defects, presumably from the manufacturing process. Topological profiles of membranes compacted with deionized (Figure 3 C) and tap water (Figure 3 D) had a consistent and homogeneous roughness and no surface defects were observed. The surface of NF270 membranes compacted with tap water (Figure 3 D) had however frequent high narrow peaks compared to the smaller peaks obtained with the DI water compaction.

Closer examination of the membrane surfaces using scanning electron microscopy revealed distinct levels of deposition depending on water grade (Figure 4). The virgin NF270 surface was relatively smooth with the presence of numerous large heterogeneities (Figure 4 A). These structures were still visible after compaction with MilliQ water (Figure 4 B). Following compaction with deionized, the membrane's surface was covered by what seemed to be a matrix layer composed of microorganisms, and biological debris and possibly organic carbon (Figure 4 C). When compacted with the DI water the large heterogeneities found on the virgin membrane were not present, and the fouling layer caused by the DI water filtration,

375 although rough in the nanoscale, was homogeneous in the microscale. In this case a
376 distinction needs to be made: although Table 2 shows similar roughness values (Rq) for the
377 membranes compacted with the MilliQ water and the DI water, in the first case the
378 membrane is very smooth with a scattered distribution of imperfections generally with
379 valley widths between 20 to 50 µm (Figure 3 A) and in the second case, although the
380 membrane is rough, it is homogeneously rough (Figure 3 B).

381 Membrane compaction using tap water led significant membrane fouling also including the
382 presence of aquatic organisms such as diatoms, small microorganisms and a pronounced
383 amount of debris (*e.g.* organic carbon) (Figure 4 D). The level of membrane fouling is
384 apprent the degree of crack artefacts observed on the membrane's surface (Figure 4 C-D)
385 caused by dehydration, especially in the case of samples compacted with tap water.

386

387 3.3 Biological assessment of NF 270 membranes after compaction using different water
388 grades.

389 The biological characteristics of the compacted NF 270 membranes was assessed by nucleic
390 acid BakLight® staining and is presented in Figure 5. Compaction using deionized and tap
391 water led to a pronounced two log difference in the total presence of microorganisms (10^7
392 cells.cm^{-2}) on the membrane compared to membranes compacted with MilliQ water after 5L
393 volume permeation (10^5 cells.cm^{-2}). A one log biological accumulation was noticeable from
394 0.5L to 5 L permeated volumes during compaction using all tested water qualities.
395 Compacted membranes using MilliQ water showed lowest counts of dead/injured
396 microorganisms throughout the compaction experiment with counts below 2×10^4 cells.cm^{-2}.

A significant increase in dead-injured cell counts was noticeable for membranes compacted with deionized and tap water only after 5L volume permeation.

3.4 Dynamic adhesion assay on compacted NF 270 membranes using different water grades.

Dynamic adhesion assays were performed on compacted membranes to establish whether permeation using different water qualities could affect the initial adhesion of *Ps. fluorescens* in terms of amount deposited on membranes and their deposition rates. Adhesion results of *Ps. fluorescens* cells conducted on compacted membranes which underwent 5 L permeation volumes of different water qualities are presented in Figure 6 and Table 3.

Different adhesion profiles were observed for *Ps. fluorescens* cells on the different compacted membranes during the 30 minutes period. Cell adhesion was highest on membranes compacted with MilliQ water after 30 minutes with 2.6×10^5 cells.cm^{-2} followed by cell deposition on membranes compacted with tap water at 1.0×10^5 cells.cm^{-2} (Figure 6). Cell deposition was lowest on membranes compacted with deionized water at 0.2×10^5 cells.cm^{-2}. The order of total cells adhered on the different surfaces after 30 min showed the following order: DI<tap<MilliQ water. The experimental data allowed maximum cell loadings on the different membranes to be deduced based on kinetic model (cf. eq.2). Membranes compacted with MilliQ water revealed highest maximum cell loadings at 2.6×10^5 cells$\times$cm^{-2}, being 5 times higher than cell loadings on membranes compacted with deionized water (Table 3). No maximum could be established after 30 minutes adhesion on membranes compacted with tap water (Figure 6) since the adhesion was still in its linear phase after 30 minutes of the experiment. However, Figure 6 clearly shows that q_{max} on membranes

compacted with tap water is higher than the q_{max} value obtained for membranes compacted with deionized water. Adhesion velocity was found to be slowest on membranes compacted with deionized water at 1.06×10^{-5} cm.min^{-1} and tap water at 3.13×10^{-5} cm.min^{-1}. *Ps. fluorescens* cells expressed highest adhesion velocities on membranes compacted with MilliQ water at 11.7×10^{-5} cm.min^{-1} (Table 3).

4 Discussion

The aim of this study was to investigate the effects of laboratory water quality during pre-compaction of nanofiltration membranes in terms of performance, surface property changes as well as its influence on standard bio-adhesion assays.

Filtration performance together with the physicochemical, physical properties and biological assessment of NF270 membrane surface were analysed at 0.5L, 2L and 5L set permeation volumes during compaction with different water sources. The dynamic bioadhesion assays were subsequently performed on the compacted NF 270 membranes using *Ps. fluorescens* cells, and experimental data was used to calculate adhesion rates as well as estimate maximum cell loadings on membranes. This allowed conclusions to be drawn about the consequential effects of laboratory water quality in membrane compaction of nanofiltration processes.

Results obtained in this study show that the water quality used during compaction of membranes, a perquisite in most membrane research laboratories, will most certainly affect membrane surface physicochemical properties prior to performing key experiments

involving bacterial adhesion. Such changes on the membrane's surface due to membrane pre-treatment might be the basis of experimental biases. Indeed, membrane compaction is in itself a form of filtration whereby the elements found in the water will end up deposited on the membrane's surface.

Membrane performance in terms of permeate flux is directly linked to water quality. The observed higher decrease of the permeate flux with increased permeated volume of tap water compared to DI and MilliQ water was caused by a higher concentration in the feed solution of organic matter, ions and dissolved solids which, not only led to the formation of a thicker fouling layer on the membrane surface, but also led to a higher osmostic pressure difference between the feed and the permeate side. In this case, a combination 446 of the cake build-up on the membrane surface and higher ionic concentration on the feed side can aggravate the permeate flux decline due to cake enhanced concentration polarisation (Hoek and Elimelech 2003). Moreover this fouling was also visible in the form of a coloration gradient as the volume of water permeated through the membrane increased: the degree of membrane coloration (yellow coloration) increased with increasing permeation volume and decreasing water purity. A study by Van der Bruggen and Vandecasteele (2001) showed that fluxmdecline during nanofiltration was predominantly caused by adsorption of organic compounds in aqueous solution onto the membrane, leading to the blocking of pores.

It might be surprising that the amount of microorganisms in DI water is higher compared to tap water, as DI water is purified tap water. However, the ion exchange resin has been found to be a good place for microorganisms to adhere onto and proliferate (Flemming 1987) for several reasons: (1) the negatively charged solutes such as TOC and other nutrients such as nitrate are removed from the water by the ion exchange resin and

consumed by the microorganisms in the resin, (2) nutrients dissolved in tap water are used by the microorganisms in the ion exchange resin as a food source and (3) the resin itself is a possible food source for bacteria as it can leach solutes to the solution.

The deposition of solutes on the membrane surface will inevitably change the membrane surface properties. The observed change in surface hydrophobicity in NF270 membranes was dependent on the water used during compaction. The NF 270 membrane, known for its hydrophilic properties (Boussu et al. (2006)), became more hydrophobic following compaction with tap and deionized water respectively. In an earlier study, Her *et al*. ((2008)) demonstrated that the levels of hydrophobic and hydrophilic fractions in Natural Organic Matter (NOM) found in water that deposited onto NF membranes determined the change in surface hydrophobicity. Likewise, the observed difference in surface hydrophobicity following compaction could have been attributed to the original fraction of hydrophilic levels of NOM found in the tested water. Interestingly, membranes compacted with deionized water having a factor 6 times less total organic carbon than tap water, were found to be most hydrophobic. This may suggest that the deionized water in this study might have contained a higher fraction of hydrophobic NOM, most likely caused by leachable residuals from the ion exchange resin of the laboratory's water purifier. Surprisingly, the biological content of the deionized water was also found to be prominent. The combination of high TOC biological levels found in deionized water might be an indication of a possible polluted and contaminated ion exchange resin. Accordingly, simple conductivity measurements should not be the sole basis for verifying the purity of deionized water. Moreover, the use of sterilized deionized water would only kill the microorganisms present, but not prevent their deposition on the membrane surface after compaction (Figure 7).

The change in surface properties following membrane compaction was sufficient to influence bacterial adhesion rates. Membranes compacted with MilliQ water attained the highest bioadhesion and adhesion velocities followed by membranes compacted with tap water and deionized respectively. Surprisingly, the extent of cell adhesion was not proportional to hydrophobicity. Despite hydrophobicity being pinpointed as one of the causes for higher adhesion onto surfaces (Lee et al. (2010), Myint et al. (2010), Subramani and Hoek (2008)), it does not in itself explain the adhesion extent of the bacteria in this study: the MilliQ water compacted membrane despite being more hydrophilic has a higher cell adhesion than the more hydrophobic surfaces of the tap and DI water compacted membranes. This indicates that surface hydrophobicity is not the sole determining factor in cell adhesion in this study and factors other than surface hydrophobicity, such as surface topology, could play more prominent role in bioadhesion. Membranes compacted with deionized and tap water, whose surfaces were covered by a fouling layer, were showed to have an unaltered surface topology compared to MilliQ water compacted membranes. The surface heterogeneities found on membranes compacted with MilliQ water might explain the observed higher bacterial adhesion compared to the smoother and more homogenous membranes following deionized and tap water compactions. A study conducted on NF 270 membranes, linked bacterial adhesion to surface heterogeneities (Subramani and Hoek 2008). Another similar study showed that surface roughness, or more specifically surface topography capable of accommodating bacterial cells, was particularly favourable for bacterial adhesion compared to other types of surface (Medilanski et al. 2002). In general, surface roughness can create conditions for the favourable initial adhesion of a single bacterium, possibly in a topological feature and this in turn forms the seed for the subsequent growth of a micro-colony. The roughness values obtained in this study were

512 performed under dehydrated compacted membranes, giving rise to high roughness readings
513 and artefacts in the form of surface cracks. However, when a specific area of 20 µm by 20
514 µm without cracks was analysed with the profilometer software, surface roughness was still
515 higher for the tap water compacted membrane (425.2 nm ± 152.9) compared to the
516 roughness obtained for DI water (164 nm ± 51.7) and MilliQ water (60.5 nm ± 17.2)
517 compacted membranes.
518 The presence of microorganisms on RO/NF membranes following compaction could lead to
519 significant degrees of bias when performing adhesion and biofouling assays. This is
520 especially important when studying biofouling using a monoculture 515 system. The
521 presence of viable organisms on freshly compacted membrane would most certainly lead to
522 the development of unanticipated outcomes.
523

524 **5 Conclusion**

525 The impact of laboratory water quality was assessed following compaction of the NF 270
526 membrane by analysing the membrane performance and surface characteristics, as well as
527 the adhesion characteristics of *P. fluorescens*. Tap and DI water compaction resulted in a
528 cake layer on the membrane surface consisting of living and dead bacteria and diatoms,
529 organic matter, dissolved solids and other components, as these were present in the water
530 used for compaction. There was a clear difference in the performance characteristics of the
531 different membranes following compaction with different water types. Compacting with DI
532 and tap water resulted in a lower permeate flux and cell adhesion rate compared to MilliQ
533 water. In contrast, compaction with MilliQ water generated the highest fluxes through the
534 membrane and a significantly higher initial adhesion of *P. fluorescens*. The reasons for the

different cell adhesion rates is difficult to elucidate due to the complexity of the tap and DI water. However, there seems to be a correlation with the topography of the surface: large heterogeneities on the surface seem to enhance *P. fluorescens* adhesion.

Overall, these results illustrate the importance of laboratory water quality in the compaction stage of NF/RO experiments and the consequent impact it has when undertaking bacterial adhesion studies. It needs to be noted while tap and DI water quality will vary significantly from laboratory to laboratory, these differences in quality can make it difficult to compare results of adhesion studies from different 537 research groups. The present study identifies the need for standardized protocols for studying membrane biofouling in laboratory conditions, particularly with respect to the water quality during membrane compaction procedures and for the feed solutions in subsequent experiments.

Acknowledgments

This research was supported by the European Research Council (ERC), project 278530, funded under the EU Framework Programme 7 and also with the financial support of Science Foundation Ireland under Grant Number "SFI 11/RFP.1/ENM/3145. The authors would like to thank Dr. Dennis Dowling and the Surface Engineering research group at UCD. We thank Dr. Ian Reid of the NIMAC microscopy platform UCD. We thank Mr. Pat O'Halloran for his invaluable technical assistance, and Mr. Liam Morris for the construction of the MFS devices.

References

Cyna, B., Chagneau, G., Bablon, G. and Tanghe, N. (2002) Two years of nanofiltration at the Méry554 sur-Oise plant, France. Desalination 147(1–3), 69-75.

Flemming, H.C. (1997) Reverse osmosis membrane biofouling. Experimental Thermal and Fluid Science 14(4), 382-391.

Ivnitsky, H., Katz, I., Minz, D., Volvovic, G., Shimoni, E., Kesselman, E., Semiat, R. and Dosoretz, C.G. (2007) Bacterial community composition and structure of biofilms developing on nanofiltration membranes applied to wastewater treatment. Water Research 41(17), 3924-3935.

Flemming, H.C. (2002) Biofouling in water systems – cases, causes and countermeasures. Applied Microbiology and Biotechnology 59(6), 629-640.

Houari, A., Seyer, D., Couquard, F., Kecili, K., Démocrate, C., Heim, V. and Martino, P.D. (2009) Characterization of the biofouling and cleaning efficiency of nanofiltration membranes. Biofouling 26(1), 15-21.

Vrouwenvelder, H.S., van Paassen, J.A.M., Folmer, H.C., Hofman, J.A.M.H., Nederlof, M.M. and van der Kooij, D. (1998) Biofouling of membranes for drinking water production. Desalination 118(1–3), 157-166.

Vrouwenvelder, J.S., Manolarakis, S.A., van der Hoek, J.P., van Paassen, J.A.M., van der Meer, W.G.J., van Agtmaal, J.M.C., Prummel, H.D.M., Kruithof, J.C. and van Loosdrecht, M.C.M. (2008) Quantitative biofouling diagnosis in full scale nanofiltration and reverse osmosis installations. Water Research 42(19), 4856-4868.

Khan, M.T., Manes, C.-L.d.O., Aubry, C. and Croué, J.-P. (2013) Source water quality shaping different fouling scenarios in a full-scale desalination plant at the Red Sea. Water Research 47(2), 558-568.

Flemming, H.C., Schaule, G., Griebe, T., Schmitt, J. and Tamachkiarowa, A. (1997) Biofouling—the Achilles heel of membrane processes. Desalination 113(2–3), 215-225.

Hijnen, W.A.M., Castillo, C., Brouwer-Hanzens, A.H., Harmsen, D.J.H., Cornelissen, E.R. and van der Kooij, D. (2012) Quantitative assessment of the efficacy of spiral-wound membrane cleaning procedures to remove biofilms. Water Research 46(19), 6369-6381.

Vrouwenvelder, J.S., Hinrichs, C., Van der Meer, W.G.J., Van Loosdrecht, M.C.M. and Kruithof, J.C. (2009a) Pressure drop increase by biofilm accumulation in spiral wound RO and NF membrane systems: role of substrate concentration, flow velocity, substrate load and flow direction. Biofouling 25(6), 543-555.

Hijnen, W.A.M., Biraud, D., Cornelissen, E.R. and van der Kooij, D. (2009) Threshold Concentration of Easily Assimilable Organic Carbon in Feedwater for Biofouling of Spiral-Wound Membranes. Environmental Science & Technology 43(13), 4890-4895.

Ivnitsky, H., Katz, I., Minz, D., Shimoni, E., Chen, Y., Tarchitzky, J., Semiat, R. and Dosoretz, C.G. (2005) Characterization of membrane biofouling in nanofiltration processes of wastewater treatment. Desalination 185(1–3), 255-268.

Huertas, E., Herzberg, M., Oron, G. and Elimelech, M. (2008) Influence of biofouling on boron removal by nanofiltration and reverse osmosis membranes. Journal of Membrane Science 318(1–2), 264-270.

Herzberg, M. and Elimelech, M. (2007) Biofouling of reverse osmosis membranes: Role of biofilm593 enhanced osmotic pressure. Journal of Membrane Science 295(1–2), 11-20.

Chong, T.H., Wong, F.S. and Fane, A.G. (2008) The effect of imposed flux on biofouling in reverse osmosis: Role of concentration polarisation and biofilm enhanced osmotic pressure phenomena. Journal of Membrane Science 325(2), 840-850.

Vrouwenvelder, J.S., Graf von der Schulenburg, D.A., Kruithof, J. 597 C., Johns, M.L. and van Loosdrecht,

607 M.C.M. (2009b) Biofouling of spiral-wound nanofiltration and reverse osmosis membranes: A feed
608 spacer problem. Water Research 43(3), 583-594.
609 Ridgway, H.F., Rigby, M.G. and Argo, D.G. (1985) Bacterial Adhesion and Fouling of Reverse Osmosis
610 Membranes. Journal of American Water Works Association 77(7), 97-106.
611 Subramani, A. and Hoek, E.M.V. (2008) Direct observation of initial microbial deposition onto
612 reverse
613 osmosis and nanofiltration membranes. Journal of Membrane Science 319(1–2), 111-125.
614 Myint, A.A., Lee, W., Mun, S., Ahn, C.H., Lee, S. and Yoon, J. (2010) Influence of membrane surface
615 properties on the behavior of initial bacterial adhesion and biofilm development onto nanofiltration
616 membranes. Biofouling 26(3), 313-321.
617 Khan, M.M.T., Stewart, P.S., Moll, D.J., Mickols, W.E., Nelson, S.E. and Camper, A.K. (2011)
618 Characterization and effect of biofouling on polyamide reverse osmosis and nanofiltration
619 membrane surfaces. Biofouling 27(2), 173-183.
620 Subramani, A., Huang, X. and Hoek, E.M.V. (2009) Direct observation of bacterial deposition onto
621 clean and organic-fouled polyamide membranes. Journal of Colloid and Interface Science 336(1), 13-
622 20.
623 Baek, Y., Yu, J., Kim, S.-H., Lee, S. and Yoon, J. (2011) Effect of surface properties of reverse osmosis
624 membranes on biofouling occurrence under filtration conditions. Journal of Membrane Science
625 382(1–2), 91-99.
626 Fonseca, A.C., Summers, R.S., Greenberg, A.R. and Hernandez, M.T. (2007) Extra-Cellular
627 Polysaccharides, Soluble Microbial Products, and Natural Organic Matter Impact on Nanofiltration
628 Membranes Flux Decline. Environmental Science & Technology 41(7), 2491-2497.
629 Miller, D.J., Araújo, P.A., Correia, P.B., Ramsey, M.M., Kruithof, J.C., van Loosdrecht, M.C.M.,
630 Freeman, B.D., Paul, D.R., Whiteley, M. and Vrouwenvelder, J.S. (2012) Short-term adhesion and
631 long-term biofouling testing of polydopamine and poly(ethylene glycol) surface modifications of
632 membranes and feed spacers for biofouling control. Water Research 46(12), 3737-3753.
633 Bernstein, R., Belfer, S. and Freger, V. (2011) Bacterial Attachment to RO Membranes Surface-
634 Modified by Concentration-Polarization-Enhanced Graft Polymerization. Environmental Science &
635 Technology 45(14), 5973-5980.
636 Suwarno, S.R., Chen, X., Chong, T.H., Puspitasari, V.L., McDougald, D., Cohen, Y., Rice, S.A. and Fane,
637 A.G. (2012) The impact of flux and spacers on biofilm development on reverse osmosis membranes.
638 Journal of Membrane Science 405–406(0), 219-232.
639 Vrouwenvelder, J.S., van Paassen, J.A.M., van Agtmaal, J.M.C., van Loosdrecht, M.C.M. and Kruithof,
640 J.C. (2009c) A critical flux to avoid biofouling of spiral wound nanofiltration and reverse osmosis
641 membranes: Fact or fiction? Journal of Membrane Science 326(1), 36-44.
642 Vrouwenvelder, J.S., Bakker, S.M., Wessels, L.P. and van Paassen, J.A.M. (2007) The Membrane
643 Fouling Simulator as a new tool for biofouling control of spiral-wound membranes. Desalination
644 204(1–3), 170-174.
645 Botton, S., Verliefde, A.R.D., Quach, N.T. and Cornelissen, E.R. (2012) Influence of biofouling on
646 pharmaceuticals rejection in NF membrane filtration. Water Research (0).

647 Khan, M.M.T., Stewart, P.S., Moll, D.J., Mickols, W.E., Burr, M.D., Nelson, S.E. and Camper, A.K.
648 (2010) Assessing biofouling on polyamide reverse osmosis (RO) membrane surfaces in a laboratory
649 system. Journal of Membrane Science 349(1–2), 429-437.
650 Lee, W., Ahn, C.H., Hong, S., Kim, S., Lee, S., Baek, Y. and Yoon, J. (2010) Evaluation of surface
651 properties of reverse osmosis membranes on the initial biofouling stages under no filtration
652 condition. Journal of Membrane Science 351(1–2), 112-122.
653 Chong, T.H., Wong, F.S. and Fane, A.G. (2007) Enhanced concentration polarization by unstirred
654 fouling layers in reverse osmosis: Detection by sodium chloride tracer response technique. Journal
655 of Membrane Science 287(2), 198-210.
656 Pang, C.M., Hong, P., Guo, H. and Liu, W.-T. (2005) Biofilm 646 Formation Characteristics of Bacterial
657 Isolates Retrieved from a Reverse Osmosis Membrane. Environmental Science & Technology 39(19),

7541-7550.
Gibbs, R.A., Scutt, J.E. and Croll, B.T. (1993) Assimilable Organic Carbon Concentrations and Bacterial Numbers in a Water Distribution System. Water Science & Technology 27(3-4), 159-166.
Vrouwenvelder, J.S., van Paassen, J.A.M., Wessels, L.P., van Dam, A.F. and Bakker, S.M. (2006) The Membrane Fouling Simulator: A practical tool for fouling prediction and control. Journal of Membrane Science 281(1–2), 316-324.
Hoek, E.M.V. and Elimelech, M. (2003) Cake-Enhanced Concentration Polarization: A New Fouling Mechanism for Salt-Rejecting Membranes. Environmental Science & Technology 37(24), 5581-5588.
Van der Bruggen, B. and Vandecasteele, C. (2001) Flux Decline during Nanofiltration of Organic Components in Aqueous Solution. Environmental Science & Technology 35(17), 3535-3540.
Flemming, H.-C. (1987) Microbial growth on ion exchangers. Water Research 21(7), 745-756.
Boussu, K., Zhang, Y., Cocquyt, J., Van der Meeren, P., Volodin, A., Van Haesendonck, C., Martens, J.A. and Van der Bruggen, B. (2006) Characterization of polymeric nanofiltration membranes for systematic analysis of membrane performance. Journal of Membrane Science 278(1–2), 418-427.
Her, N., Amy, G., Chung, J., Yoon, J. and Yoon, Y. (2008) Characterizing dissolved organic matter and evaluating associated nanofiltration membrane fouling. Chemosphere 70(3), 495-502.
Medilanski, E., Kaufmann, K., Wick, L.Y., Wanner, O. and Harms, H. (2002) Influence of the Surface Topography of Stainless Steel on Bacterial Adhesion. Biofouling 18(3), 193-203.

List of Tables

692 **List of Figures**

693 Figure 1 MFS Cross-Flow system.

694

695 Figure 2 Flux decline of the NF 270 membrane during compaction with different water
696 sources (0.5, 2 and 5 L of source water filtered, 0.66 L.min^{-1} 690 in each MFS, 15 bar and
697 21°C). Each experiment was repeated twice. The error bar represents the variability of the
698 flux obtained for all the membranes used in duplicate exposed to that particular permeate
699 volume (0.5, 2 and 5 L).

700

701 Figure 3 Height topography of a compacted membrane with MilliQ (A), DI (B) and tap
702 water(C) were obtained by optical profilometery (223×293 µm). The 2D images associated
703 to each profile are shown, all X and Y axes are in microns.

704

705 Figure 4 Scanning electron micrographs of non-compacted NF 270 membranes (A) and
706 compacted NF270 membranes after 5L permeated volumes of Milli Q water (B), deionized
707 water (C), and tap water (D) at 0.66 L•min^{-1}, 15 bar and 21°C .

708

709 Figure 5 Number of accumulated microorganisms on NF270 membranes following
710 compaction with increasing permeated volumes of different water qualities. Error bars
711 represent standard error.

712

713 Figure 6 Dynamic adhesion of *Ps. fluorescens* cells on compacted NF-270 membranes after
714 5L permeated volumes of different water qualities.

715

716 Figure 7 Fluorescence micrographs showing membrane samples following membrane
717 compaction with autoclaved DI water at 15 bar stained with (A) Syto 9 and (B) Propidium
718 Iodide and membrane compaction with non-autoclaved DI water at 15 bar stained with (C)
719 Syto 9 and (D) Propidium Iodide

720

721 Table **1**

Water Quality	MilliQ Water	Deionized Water	Tap Water
Total Solids ($mg \cdot L^{-1}$)	ND*	ND*	109.17 ± 5.2
pH	6.01 ± 0.11	6.31 ± 0.29	7.44 ± 0.07
TOC ($mg \cdot C \cdot L^{-1}$)	0.04 ± 0.04	1.6 ± 0.7	9.6 ± 0.8
Conductivity ($\mu S \cdot cm^{-1}$)	0.4 ± 0.1	4 ± 2	168 ± 7
Culturable counts ($Cells \cdot mL^{-1}$)	ND*	239	1.4
Total cell counts (10^3 $Cells \cdot mL^{-1}$)	1 ± 1	1472 ± 421	123 ± 47
Total dead/injured counts (10^3 $Cells \cdot mL^{-1}$)	3 ± 2	2020 ± 482	82 ± 44

722 *ND: not detected

723

724

725

726

Table **2**

		Compacted NF 270 membranes								
		MilliQ water			Deionized water			Tap water		
	Permeated volume	0.5L	2L	5L	0.5L	2L	5L	0.5L	2L	5L
Contact angle	Θ_{water}	40.5 ± 1.11	45.5 ± 0.89	49.7 ± 0.58	55.7 ± 0.34	64.3 ± 0.45	68.9 ± 0.63	45.8 ± 0.9	53.4 ± 0.6	56.0 ± 3.9
	$\Theta_{diiodomethane}$	36.6 ± 0.41	36.9 ± 0.88	34.4 ± 0.67	45.3 ± 0.56	46.8 ± 0.88	44.6 ± 0.97	38.6 ± 0.7	36.4 ± 1.6	28.7 ± 6.7
	$\Theta_{ethylene\ glycol}$	28.9 ± 0.98	25.8 ± 0.73	26.6 ± 0.42	34.6 ± 0.64	41.5 ± 0.81	47.8 ± 0.59	32.9 ± 0.9	36.7 ± 0.7	40.6 ± 5.6
Surface tension ($mJ \cdot m^{-2}$)	γ^{LW}	41.4 ± 0.18	41.3 ± 0.41	42.3 ± 0.33	36.9 ± 0.31	35.7 ± 0.51	37.0 ± 0.56	40.3 ± 0.4	41.9 ± 0.7	45.5 ± 0.5
	γ^{-}	49.1 ± 1.83	44.8 ± 1.4	33.7 ± 0.99	28.5 ± 0.55	19.9 ± 0.85	17.8 ± 1.24	44.9 ± 1.4	35.5 ± 1.2	33.4 ± 1.2
	γ^{+}	0.1 ± 0.04	0.04 ± 0.01	0.03 ± 0.01	0.1 ± 0.02	0.2 ± 0.04	0.08 ± 0.02	0.15 ± 0.05	0.19 ± 0.04	0.55 ± 0.1
	γ^{AB}	4.06 ± 0.6	2.22 ± 0.4	1.86 ± 0.32	3.9 ± 0.4	4.9 ± 0.6	2.77 ± 0.4	3.94 ± 0.73	4.80 ± 0.8	9.1 ± 0.9
	γ^{S}	53.2 ± 2.3	47.0 ± 1.65	35.6 ± 1.03	32.5 ± 0.4	24.8 ± 0.7	20.6 ± 1.32	48.9 ± 1.9	40.3 ± 1.8	42.6 ± 2.04
Surface roughness (RMS) (nm)	200 µm x 200 µm surface area*	468 ± 142	417 ± 121	511 ± 143	452 ± 177	592 ± 144	562 ± 123	521 ± 160	695 ± 251	1166 ± 147

* Roughness deduced from surface profilometry.

Table **3**

	Compacted NF 270 membranes		
	MilliQ water	Deionized water	Tap water
Estimated maximum cell loading q_{max} (10^4 Cells • cm^{-2})	26 ± 2.5	5.2 ± 1.3	ND
Adhesion velocity k_d(10^{-5} cm•min^{-1})	11.7 ± 2.4	1.06 ± 0.09	3.13 ± 0.3

*ND: not determined.

1 Figure **1**

2

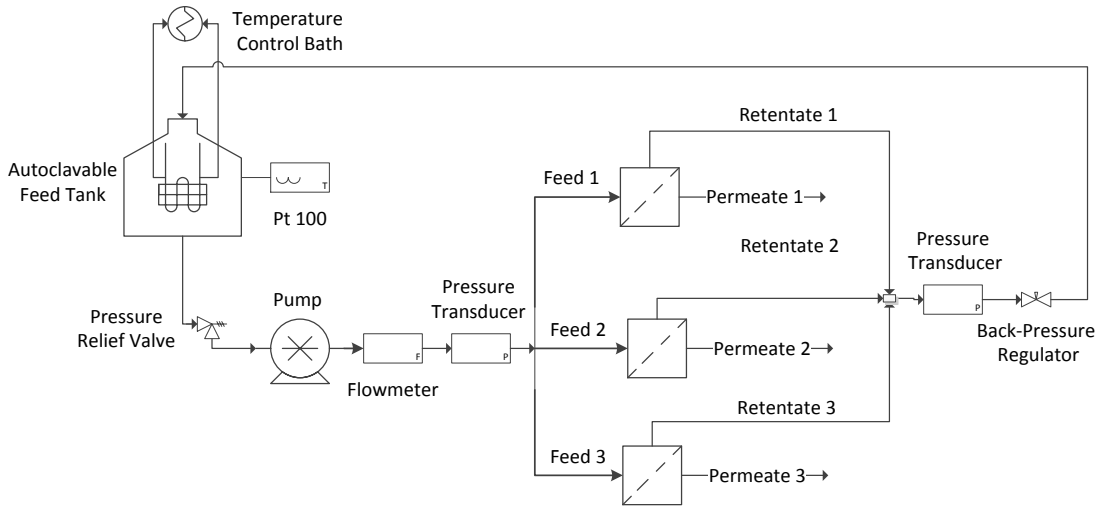

3

4

Figure 2

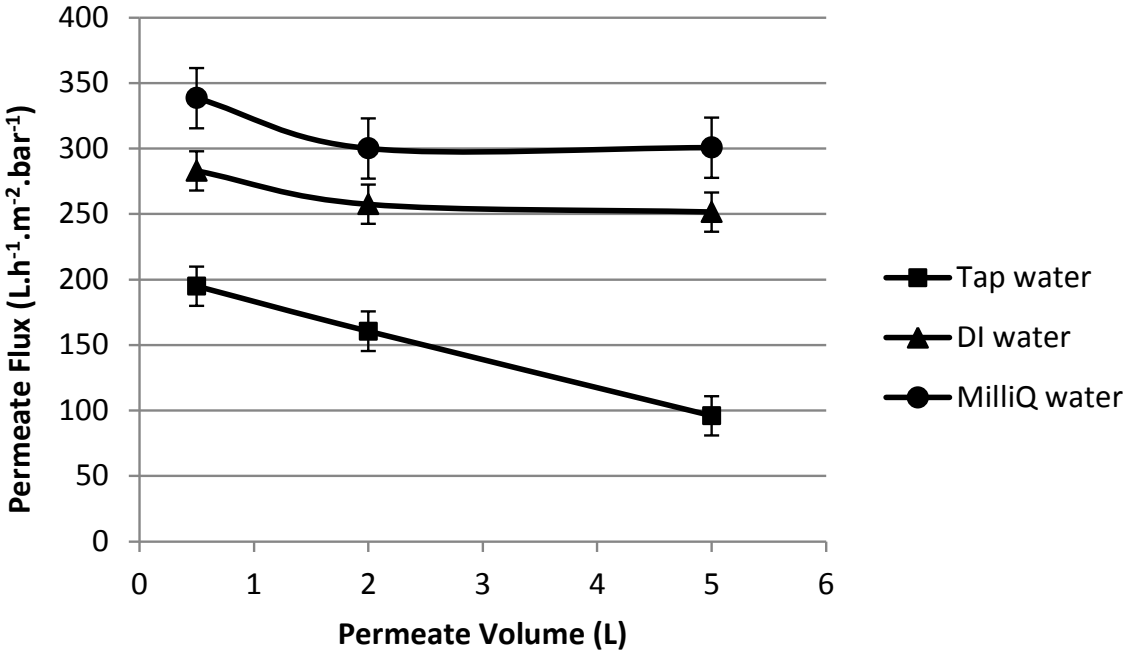
400
350
300
250
200
150
100
50
0
0
1
2
3
4
5
6
Permeate Flux (L.h-1.m-2.bar-1)
Permeate Volume (L)
Tap water
DI water
MilliQ water

Figure **3**

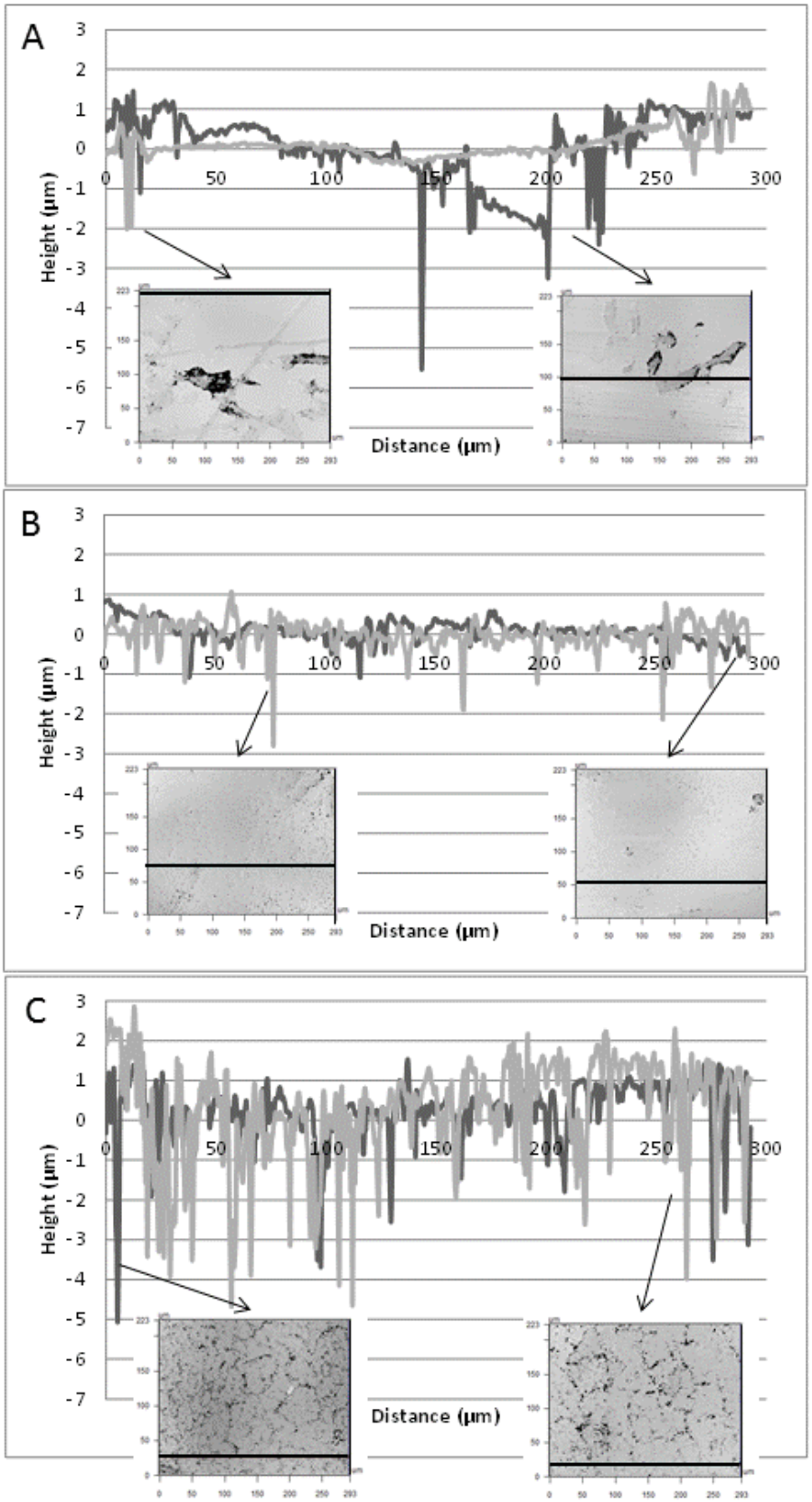
A
B
C
Height (µm)
Distance (µm)
3
2
1
0
-1
-2
-3
-4
-5
-6
-7
0
50
100
150
200
250
300

Figure **4**

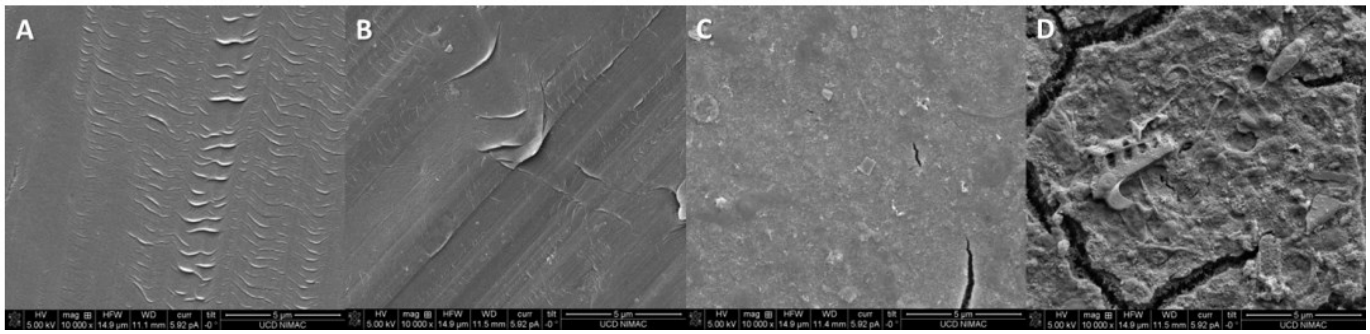

Figure **5**

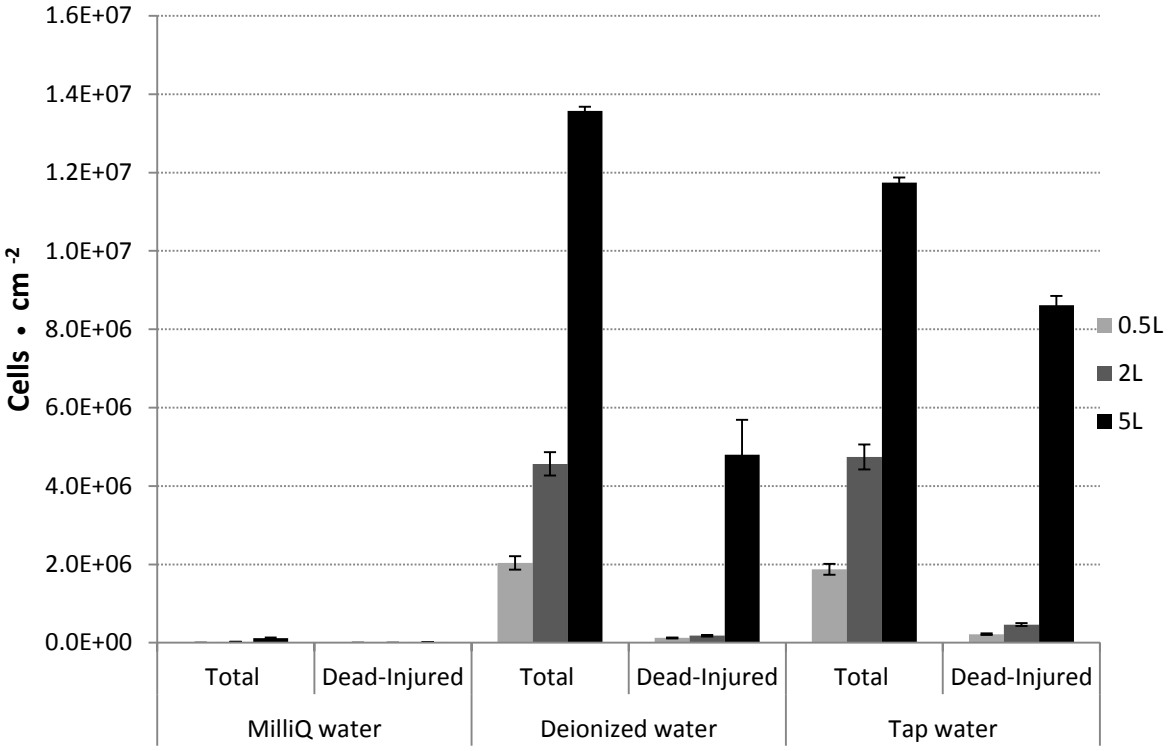
1.6E+07
1.4E+07
1.2E+07
1.0E+07
8.0E+06
6.0E+06
4.0E+06
2.0E+06
0.0E+00
Cells • cm -2
0.5L
2L
5L
Total
Dead-Injured
Total
Dead-Injured
Total
Dead-Injured
MilliQ water
Deionized water
Tap water

Figure **6**

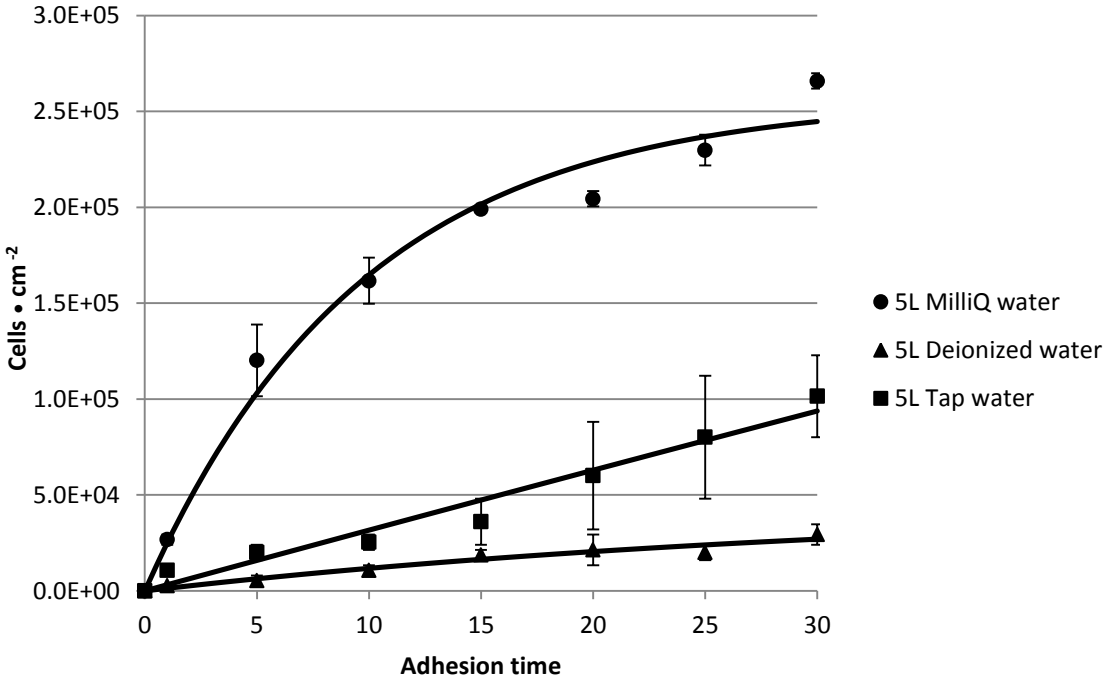
3.0E+05
2.5E+05
2.0E+05
1.5E+05
1.0E+05
5.0E+04
0.0E+00
Cells • cm -2
0
5
10
15
20
25
30
Adhesion time
5L MilliQ water
5L Deionized water
5L Tap water

1 Figure 7

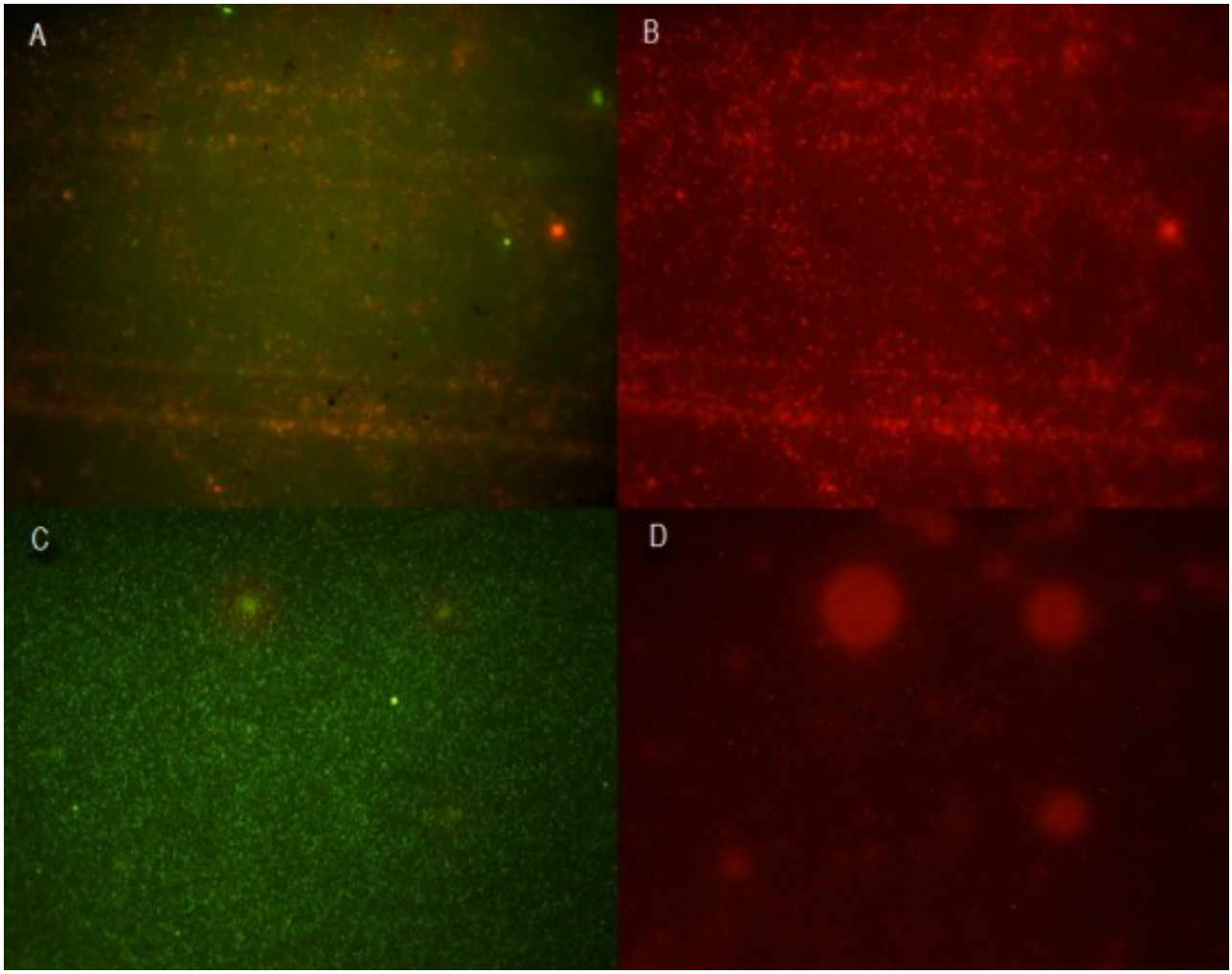

2